PPPL-2256

UC20-A,B,G

PPPL-2256

MAGNETIC ISLANDS AT THE FIELD REVERSAL SURFACE IN REVERSED FIELD PINCHES

By

R.I. Pinsker and A.H. Reiman

SEPTEMBER 1985

PLASMA PHYSICS LABORATORY

PRINCETON UNIVERSITY

PRINCETON, NEW JERSEY

PREPARED FOR THE U.S. DEPARTMENT OF ENERGY, UNDER CONTRACT DE-AC02-76-CHO-3073

PPPL--2256

DE86 000590

Magnetic Islands at the Field Reversal Surface in Reversed Field Pinches

R. I. Pinsker and A. H. Reiman
Plasma Physics Laboratory, Princeton University
Princeton, NJ 08544

In the reversed field pinch (RFP), magnetic field perturbations having zero poloidal mode number and any toroidal mode number are resonant at the field reversal surface. Such perturbations are a particular threat to the RFP because of their weak radial dependence at low toroidal mode number, and because the toroidal field ripple is essentially of this type. The widths of the resulting islands are calculated in this paper. The self-consistent plasma response is included through the assumption that the plasma relaxes to a Taylor force-free state. The connection with linear tearing mode theory is established for those limits where arbitrarily large islands result from infinitesimal perturbations. Toroidal effects are considered, and application of the theory to RFP experiments is discussed.

I. INTRODUCTION

Over the past decade, the reversed field pinch (RFP) has emerged as one of the leading alternative concepts in the world fusion program. Its low value of q promises improved reactor economics because of the relatively large ohmic heating power available and because of the relatively small toroidal field required. Experimentally, RFP's have demonstrated the capability to maintain themselves in a macroscopically stable reversed field state for time scales long compared to the resistive diffusion time of the field reversed layer.[1]

A potential concern about the RFP is its vulnerability to field errors having zero poloidal mode number. The magnetic surface where $q = 0$ (the field reversal surface) resonates with perturbations having $m = 0$ and arbitrary n, where m and n are the poloidal and toroidal mode numbers. At large aspect ratio, the scalar potential for the magnetic field errors has a radial dependence of approximately $I_m(n\rho/R)$, where R is the major radius, ρ is the cylindrical radial coordinate, and I is a modified Bessel function.[2] In particular, the radial component of the $m = 0$ field error has an approximately linear ρ dependence for $\rho \ll R/n$. Even more serious, the toroidal field ripple is largely $m = 0$, so that the toroidal field coils themselves directly drive a resonant perturbation. The ripple is an unavoidable consequence of the discreteness of the toroidal field coils. Reducing the magnitude of this ripple in a large device is expensive, so that it is important to understand the consequences of a given level of field ripple.

A resonant $m = 0$ field produces an island on the field reversal surface. The effect on confinement is deleterious, since the pressure is constant on the separatrix; when the island width becomes sufficiently large that the separatrix intersects the liner (or limiter), confinement is lost throughout the field reversal region, and field reversal cannot be sustained. Experimentally, field ripple and other field errors have been shown to result in poor confinement in ZT–40M.[3]

In this paper, we calculate the width of the islands at the field reversal surface in the presence of external $m = 0$ field perturbations. This may be regarded as a three-dimensional equilibrium problem. The external field perturbations are present at the outset, and the plasma relaxes to equilibrium in their presence. To determine the self-consistent plasma current, we assume that the plasma relaxes to a force-free state,

$$\nabla \times \mathbf{B} = \lambda \mathbf{B} \,, \tag{1}$$

with λ a constant. This is consistent with the premise that the plasma relaxes to a state of minimum energy subject to conservation of total magnetic helicity and toroidal flux,[4,5] an ansatz that has had great success in interpreting the behavior of the RFP. Previously published analyses of field errors in RFPs have not included the self-consistent effect of the plasma.[6,7] In certain limits of the parameters, the self-consistent plasma response results in unbounded island

widths for finite-sized perturbations. In these cases, the consistency of our approach with the conventional linear tearing mode theory is demonstrated.

The plan of the paper is as follows. In Sec. II we use a large aspect ratio (cylindrical) approximation. We match a vacuum field corresponding to a fixed external $m = 0$ perturbation with the field inside the plasma given by Eq. (1), and we obtain an explicit expression for the island width at the $q = 0$ surface. The self-consistent plasma response, but not the external perturbation, is constrained by the presence of a conducting wall in the vacuum region. We find that the plasma currents generally enhance the island growth.

To complete our picture of the plasma response to $m = 0$ perturbations, in Sec. III we perform a linearized $m = 0$ stability analysis in the cylinder for both resistive and ideal modes. We include the effect of a conducting wall in the vacuum region. We discuss the connection between our stability results and our island width calculation.

In Sec. IV, we check the cylindrical approximation by numerically following field lines in an analytic nonaxisymmetric force-free toroidal equilibrium. We make use of the fact that Eq. (1) is linear, so that its general three-dimensional solution can be written explicitly as a superposition of solutions obtained by separation of variables. We find that the finite aspect ratio corrections to the island width are of the order of the inverse aspect ratio, so that the cylindrical approximation is a good one.

The theory is applied to RFP experiments in Sec. V. We find that the islands driven by toroidal ripple are a significant effect which must be taken into account in designing an RFP.

II. $m = 0$ ISLANDS

We calculate the widths of the islands due to the presence of nonaxisymmetric $m = 0$ field errors. This is a three-dimensional equilibrium problem; the plasma forms in the presence of the magnetic field perturbations, so that the islands are present when the plasma reaches equilibrium. The island width is affected by the current flowing in the plasma, and the plasma current distribution is in turn affected by the presence of the island. We take the self-consistent magnetic field in the plasma to be described by Eq. (1), with λ constant in the plasma region. This form for the magnetic field follows from the assumption that the plasma relaxes to a state of minimum energy subject to the conservation of total magnetic helicity and toroidal flux. The experimentally observed maintenance of field reversal on time scales long compared to the resistive diffusion time of the field reversed layer,[1] presumably due to ongoing turbulent reconnection, makes this a plausible model. The model predicts the onset of field reversal as the toroidal current is increased, and gives a reasonably good prediction of the actual magnitude of the toroidal field at the edge as a function of the toroidal current (the so-called "F-θ curve"). The predictions of the model

are also consistent with the threshold for the $m = 1$ resistive internal kink mode given by a linearized stability analysis.[8]

Equation (1) is a necessary, but not a sufficient, condition for minimum energy. To supplement our calculation of the $m = 0$ island widths, we therefore do a stability analysis for $m = 0$ modes in Sec. III. We will see that the results of the stability analysis are consistent with our model, in that the island width predicted by Eq. (1) for a fixed external perturbation diverges as the stability boundary is approached. That is, the response to a driving term (the nonaxisymmetric field error) becomes infinite when the plasma goes unstable. The solutions that we construct are still not necessarily true minimum energy states, as they could be unstable to modes having nonzero m. We have not attempted to include the effects of $m \neq 0$ perturbations in our analysis. Our interest in this paper is to determine the plasma response to field errors which resonate with the field reversal surface, and particularly to the toroidal field ripple. It is not our intention here to do an extensive stability analysis. For those cases where we find unacceptably large island widths, there is cause for concern about the effects of the $m = 0$ field errors. For those cases where we find small island widths, the stability to $m \neq 0$ modes remains to be verified.

In this section we use an infinite aspect ratio (cylindrical) approximation. In Sec. IV we will see that this is a good approximation. The cylindrically symmetric solution to Eq. (1) is $\mathbf{B}_o = \mathrm{B}_o(\mathrm{J}_1(w)\hat{\theta}_c + \mathrm{J}_0(w)\hat{\phi})$, where we have introduced a cylindrical coordinate system (ρ, θ_c, ϕ) and defined the dimensionless radial variable $w = \lambda\rho$. This is the equilibrium in the absence of nonaxisymmetric perturbations. Since we analyze only $m = 0$ perturbations, θ_c remains an ignorable coordinate, and flux functions ψ and ψ_v exist for the perturbed plasma and vacuum fields, respectively, in terms of which

$$\mathbf{B} = \nabla\psi \times \nabla\theta_c \quad + \quad \rho \mathrm{B}_{\theta_c} \nabla\theta_c \quad .$$

We find the form of ψ in the plasma by solving Eq. (1) in a cylinder,[4] retaining only the $m = 0$ solutions, and constructing the flux function

$$\psi(\rho, \phi) = \sum_{n=0}^{\infty} \frac{\epsilon_n}{\kappa_n} \rho \mathrm{J}_1(\kappa_n \rho) \cos n\phi \ , \tag{2}$$

where $\kappa_n = \left|\lambda^2 - n^2/R^2\right|^{\frac{1}{2}}$, and $\mathrm{J}_1(\kappa_n\rho)$ is to be replaced by $\mathrm{I}_1(\kappa_n\rho)$ if $\lambda^2 R^2 < n^2$. Note that $\epsilon_0 = \mathrm{B}_o$ and $\kappa_0 = \lambda$. If we allow for a perturbation with a particular toroidal mode number n in Eq. (2), expanding ψ around the field reversal surface $\rho = \rho_0$ yields a half-width for the $m = 0$ islands of

$$[\Delta\rho]_{max.} = \left(\frac{2}{\lambda\kappa_n} \frac{\epsilon_n}{\mathrm{B}_o} \frac{|\mathrm{J}_1(\kappa_n\rho_0)|}{\mathrm{J}_1(j_{0,1})} \right)^{\frac{1}{2}} \ , \tag{3}$$

where the first zero of the J_0 Bessel function is $j_{0,1} = 2.40482\ldots$ and the radius of the $q = 0$ surface is $\rho_0 = j_{0,1}/\lambda$.

To complete the calculation, we must relate the perturbation amplitude within the plasma to the size of the vacuum error field. We consider first the case where there is no conducting wall. The flux function in the vacuum is

$$\psi_v = C + \frac{1}{2}\rho^2 B_T + \sum_{n=1}^{\infty} \left[\alpha_n K_1(k_n\rho) + \beta_n I_1(k_n\rho)\right] \frac{\rho \cos n\phi}{k_n} , \qquad (4)$$

where $k_n = n/R$ and I_1, K_1 are the modified Bessel functions of the first and second kind, respectively. In Eq. (4) the K_1 terms represent the contribution to the vacuum magnetic field due to the plasma currents, and the I_1 terms represent the "applied" $m = 0$ error field, due to currents outside the plasma. We normalize the amplitude of the applied $m = 0$ component of the vacuum field $\beta_n = b_1/I_1(k_n\rho_e)$, where the plasma edge is at radius ρ_e. (Note that $\rho_e > j_{0,1}/\lambda$ for field reversal.) With this normalization, the applied radial field at ρ_e is just $B_{1\rho}(\rho_e) = b_1 \sin n\phi$. We solve for the "scattered" and "transmitted" field amplitudes α_n and ϵ_n in terms of the known "incoming" amplitude β_n by applying matching conditions on the perturbed plasma boundary.

Specifically, we match the values of ψ and ψ_v and the normal derivatives $\hat{n} \cdot \nabla\psi$ and $\hat{n} \cdot \nabla\psi_v$ across the perturbed boundary. (This is equivalent to matching the radial and tangential components of the magnetic field.) In terms of ϵ_n, the perturbed boundary is found to be

$$\rho = \rho_e - \frac{\epsilon_n}{B_o} \frac{J_1(\kappa_n\rho_e)}{J_0(\lambda\rho_e)} \frac{\cos n\phi}{\kappa_n} ,$$

which gives a normal vector to first order:

$$\hat{n} = \hat{\rho} - \hat{\phi} \frac{\epsilon_n}{B_o} \frac{J_1(\kappa_n\rho_e)}{J_0(\lambda\rho_e)} \frac{n}{\kappa_n R} \sin n\phi .$$

Then ψ on the perturbed boundary is

$$\psi(\text{perturbed boundary}) = \psi_o(\rho_e) + \psi_1(\rho_e) + \left[\frac{d\psi_o}{d\rho}\right]_{\rho_e} (\rho - \rho_e) + \ldots .$$

Setting this equal to the analogous expression for ψ_v(perturbed boundary) yields a zero-order and a first-order matching condition. Matching $\hat{n} \cdot \nabla\psi$ to $\hat{n} \cdot \nabla\psi_v$ on the perturbed boundary in the same way gives a second pair of conditions. Eliminating α_n between the two first-order conditions produces the desired result

$$\epsilon_n = b_1 \frac{K_0 + (I_0/I_1)K_1}{(\frac{n}{\kappa_n R})K_0 J_1(\kappa_n \rho_c) + K_1 \left\{ J_0(\kappa_n \rho_c) + (\frac{\lambda}{\kappa_n}) J_1(\kappa_n \rho_c) J_1(\lambda \rho_c)/J_0(\lambda \rho_c) \right\}} , \tag{5}$$

in which the argument of the modified Bessel functions is $k_n \rho_c$, and $J_0(\kappa_n \rho_c)$, $J_1(\kappa_n \rho_c)$ are to be replaced by $I_0(\kappa_n \rho_c), I_1(\kappa_n \rho_c)$ if $\lambda^2 R^2 < n^2$. Substituting Eq. (5) into Eq. (3) gives the final result for the $m = 0$ island width in terms of the dimensionless measure of ripple in the vacuum field, b_1/B_o. In Sec. V we will calculate the magnitude of the ripple due to the discreteness of the toroidal field coils.

Next we include the effect of a conducting wall at radius ρ_w . We expect that the error field, like the toroidal field and other ambient magnetic fields, is present on a time scale long compared to the L/R time of the conducting wall. We therefore assume that the field ripple has "soaked through" the conducting shell when the plasma forms, while the plasma response is on a time scale short compared to the resistive time of the shell. [For discharges lasting longer than the shell's resistive time, the island width approaches the value given by Eqs. (3) and (5).] On the short time scale, the flux function in the vacuum becomes

$$\psi_v = C + \frac{1}{2}\rho^2 B_T + \sum_{n=1}^{\infty} \left\{ \alpha_n \left[K_1(k_n \rho) - \frac{K_1^w}{I_1^w} I_1(k_n \rho) \right] + \beta_n I_1(k_n \rho) \right\} \frac{\rho \cos n\phi}{k_n},$$

in which functions with the superscript w are evaluated at $n\rho_w/R$. The term multipiying α_n now includes not only the effect of the plasma currents, but also the contribution to the field due to the induced wall currents. This term is constrained to vanish at the wall. The calculation of the "transmitted" field amplitude ϵ_n proceeds as before. We can obtain the results by replacing K_0, K_1 in Eq. (5) according to the prescription

$$K_0(k_n \rho_c) \rightarrow K_0(k_n \rho_c) + \frac{K_1^w}{I_1^w} I_0(k_n \rho_c) \quad , \quad K_1(k_n \rho_c) \rightarrow K_1(k_n \rho_c) - \frac{K_1^w}{I_1^w} I_1(k_n \rho_c).$$

As the wall radius becomes much larger than the plasma edge radius, we recover Eq. (5). As the wall radius approaches the plasma edge, we find that the island width approaches the width one would obtain ignoring the self-consistent effect of the plasma. In this limit, the self-consistent plasma current gets vanishingly small.

We can quantify the plasma effect on the perturbation at the $q = 0$ surface by defining an amplification factor A as follows:

$$A \equiv \frac{\mathrm{B}_{1\rho}(\rho_0) \quad \text{as calculated above}}{\mathrm{B}_{1\rho}(\rho_0) \text{ if the plasma were absent}}$$
$$= \frac{\epsilon_n (k_n/\kappa_n) \mathrm{J}_1(\kappa_n \rho_0)}{b_1 \left[\mathrm{I}_1(k_n \rho_0)/\mathrm{I}_1(k_n \rho_e) \right]}.$$

In Figs. 1–3, we plot the amplification factor A as a function of the pinch parameter[9]

$$\Theta \equiv \mathrm{B}_{c\theta_e}(\rho_e)/(\mathrm{B}_{c\phi}) = \frac{1}{2}\lambda \rho_e.$$

We take $R/\rho_e = 5.7$ (the aspect ratio of ZT-40M). For Figs. 1 and 2 we have taken the conducting wall at infinity, with toroidal mode numbers $n = 20$ and $n = 72$, respectively. For Fig. 3 we have taken the wall at $\rho_w = 1.05\rho_e$, with $n = 20$. The pinch parameter in these figures ranges from that for which field reversal occurs ($\Theta = \frac{1}{2} j_{0,1} = 1.202\ldots$) to $\Theta = 1.56$. At the latter value of Θ the cylindrically symmetric equilibrium becomes unstable to an internal kink mode. The shaded regions in Figs. 1–3 represent $m = 0$ unstable regimes. They will be discussed in Sec. III.

It is apparent from Figs. 1–3 that the effect of the self-consistent plasma currents is to magnify the vacuum islands, rather than to "heal" them. (The latter effect would be represented by $A < 1$.) The self-consistent plasma effect can be quite important. In particular, the amplification factor (and therefore the island width) diverges as we approach the value of Θ for which the denominator of Eq. (5) vanishes. The response to the nonaxisymmetric driving term becomes singular at this value of Θ. This corresponds to the onset of a tearing mode. A solution to the equations having $\beta_n = 0$ represents a marginally stable tearing eigenmode. In the following section we determine the stability to $m = 0$ perturbations.

III. STABILITY TO $m = 0$ PERTURBATIONS

In this section we complete our picture of the plasma response to $m = 0$ perturbations by determining the stability of the cylindrically symmetric plasma to resistive and ideal $m = 0$ modes, including the effect of a conducting wall in the vacuum region. For parameters corresponding to Figs. 1–3, the calculations will determine the ideal and resistive unstable regions indicated in those figures.

In the resistive stability analysis, the equation governing the outer solution is, in fact, precisely Eq. (1). The equations are the same as those we have already solved, but the boundary conditions are somewhat different. Only the radial component of the magnetic field is now continuous across the rational surface, but the radial component of the magnetic field is constrained to vanish at the conducting wall. The plasma region is divided into an interior region,

$0 < \rho < \rho_0$, in which the flux function is given by Eq. (2), and a reversed field region $\rho_0 < \rho < \rho_e$ in which

$$\psi_r = \sum_{n=0}^{\infty} \left[\delta_n J_1(\kappa_n \rho) + \gamma_n N_1(\kappa_n \rho) \right] \frac{\rho \cos n\phi}{\kappa_n} . \tag{6}$$

Again, the Bessel functions of the first and second kinds in Eq. (6) are to be replaced by their modified counterparts if $\lambda^2 R^2 < n^2$, according to the rule

$$J \rightarrow I, \quad N \rightarrow -(2/\pi)K ,$$

where the constant has been chosen to make the functions continuous in the neighborhood of the transition.

We consider first the case where there is no conducting wall. The vacuum field flux function is then given by Eq. (4) with $\beta_n = 0$, since the magnetic field must vanish at infinity. The matching of ψ to ψ_r at $\rho = \rho_0$ now supplements the two matching conditions across the perturbed boundary, and these three conditions together determine

$$\Delta' \equiv \frac{\psi_r'(\rho_0) - \psi'(\rho_0)}{\psi(\rho_0)} .$$

At marginal stability, $\Delta' = 0$. After a little algebra, we find that $\Delta' = 0$ gives precisely the denominator of Eq. (5) set equal to zero. It is clear that this must be the case, because at $\Delta' = 0$ the magnetic field is continuous across the rational surface. We then get a solution to the equations and boundary conditions of the previous section with $\beta_n = 0$.

The stability diagram for $m = 0$ tearing modes with $R/\rho_e = 5.7$ is shown in Fig. 4. For $n \gg j_{0,1}(R/\rho_e)$, we can use the large argument asymptotic expansions of the modified Bessel functions to obtain an approximate expression for the marginal point, where Δ' vanishes:

$$n_{crit} \sim -\frac{J_1(2\Theta)}{J_0(2\Theta)} \left(\frac{R}{\rho_e} \right) \Theta .$$

This expression is also shown in Fig. 4. Taylor expanding this around $2\Theta = j_{0,1}$, we get a rough estimate for the Θ value at which a particular n goes unstable: $\Theta_n \simeq j_{0,1} n / \left[2n - (R/\rho_e) \right]$. For the examples of Figs. 1 and 2, $\Theta_{20} \simeq 1.402$ and $\Theta_{72} \simeq 1.252$, which are in good agreement with the numerically obtained $\Theta_{20} = 1.4050$ and $\Theta_{72} = 1.2512$.

To treat a conducting wall at $\rho = \rho_w$, we choose β_n in Eq. (4) so that $\psi_v(\rho = \rho_w) = 0$. We obtain the generalized marginal stability condition:

$$\Big[\frac{\lambda}{\kappa_n}\frac{J_1(\lambda\rho_e)}{J_0(\lambda\rho_e)}\{K_1^{ve}-\frac{K_1^w}{I_1^w}I_1^{ve}\}+(\frac{n}{\kappa_n R})\{K_0^{ve}+\frac{K_1^w}{I_1^w}I_0^{ve}\}\Big]J_1^e$$
$$+\{K_1^{ve}-\frac{K_1^w}{I_1^w}I_1^{ve}\}I_0^e=0\,, \qquad (7)$$

in which functions with a superscript e are evaluated at $\kappa_n\rho_e$ and are to be replaced with their modified counterparts as before if $n^2>\lambda^2R^2$, and functions with the superscript ve are evaluated at $n\rho_e/R$. Equation (7) reduces to the denominator of Eq. (5) set equal to zero as ρ_w/ρ_e becomes much greater than unity, and reduces to the expression for marginal stability given in Ref. 8 as $\rho_w/\rho_e\to 1$.

In Ref. 8 , the tearing mode stability of the cylindrically symmetric Bessel function equilibrium with a conducting wall at $\rho=\rho_e$ was analyzed, and it was shown that $m=0$ modes are stable for $\Theta<1.916$. The stability diagram shown in Fig. 5 illustrates the transition from the close wall case of Ref. 8 to the distant wall case. The dotted lines are the marginal points $\Delta'=0$ for three ratios of the conducting wall radius to the plasma edge radius $\rho_w/\rho_e=1.0,\ 1.15,\ \infty$. The expression for Δ' also exhibits singularities, indicating a transition to ideal instability.

The ideal stability is determined by Newcomb's criterion.[10] For our case, this stability criterion reduces to the condition that the flux function calculated above not vanish in the plasma. In Figs. 1–3, the corresponding ideally unstable regions are shown. In each case, as Θ is decreased the cylindrically symmetric equilibrium first becomes unstable to resistive modes, and then to ideal modes. The width of the resistive instability region decreases as n decreases.

IV. TOROIDAL EFFECTS

In Sec. II, we used a cylindrical approximation to calculate the width of the $m=0$ islands. To check the validity of this approximation for tori of reasonable aspect ratio, we next use a class of fully three-dimensional equilibria which are analytic solutions of $\nabla\times\mathbf{B}=\lambda\mathbf{B}$. We consider a solution with a particular toroidal mode number, and compare the island width at the field reversal surface predicted by the simplest cylindrical approximation with the width found by numerical field line following.

We introduce a spherical coordinate system (r,θ,ϕ) in which the coordinates of the magnetic axis are $(R_{ax},\pi/2,\phi)$ and the symmetry axis of the equilibrium has $\theta=0,\pi$. Then the general solution of $\nabla\times\mathbf{B}=\lambda\mathbf{B}$ is given in Ref. 11 as

$$\mathbf{B} = \sum_{n=0}^{\infty}\sum_{k=n}^{\infty} \epsilon_{nk}\exp(in\phi)\left\{\left[k(k+1)\mathrm{P}_k^n(\mu)\frac{j_k(u)}{u}\right]\hat{r}\right.$$
$$+ \left[\frac{in}{\sin\theta}\mathrm{P}_k^n(\mu)j_k(u) - \sin\theta\frac{d\mathrm{P}_k^n(\mu)}{d\mu}\frac{1}{u}\frac{d}{du}\left(uj_k(u)\right)\right]\hat{\theta}$$
$$\left. + \left[\sin\theta\frac{d\mathrm{P}_k^n(\mu)}{d\mu}j_k(u) + \frac{in}{\sin\theta}\mathrm{P}_k^n(\mu)\frac{1}{u}\frac{d}{du}\left(uj_k(u)\right)\right]\hat{\phi}\right\}, \qquad (8)$$

where $\mu = \cos\theta$ and the normalized radial coordinate $u \equiv \lambda r$. For axisymmetric solutions ($n = 0$) , the flux function ψ_0 is exactly

$$\psi_0(u,\theta) = \sum_{k=1}^{\infty} \epsilon_k u j_k(u)\sin^2\theta\frac{d\mathrm{P}_k(\mu)}{d\mu}.$$

At a magnetic axis ψ_0 is an extremum.

For comparison with the cylindrical approximation, we obtain large aspect ratio axisymmetric equilibria by adding three terms in the series above with different k's: $k = k_1, k_2, k_3$ (with $n = 0$). We set ϵ_{k_3} to unity, and consider only odd k's, which yield up–down symmetry around the midplane. For comparison with Sec. II, we are interested in axisymmetric solutions having nearly circular flux surfaces. Fix ϵ_{k_2} to be some particular value. Then solve the following two conditions simultaneously:

1) $\left.\dfrac{\partial\psi_0}{\partial u}\right]_{u=u_{ax},\theta=\pi/2} = 0$; determines magnetic axis position

2) $\left.\dfrac{\partial^2\psi_0}{\partial x^2}\right]_{axis} = \left.\dfrac{\partial^2\psi_0}{\partial z^2}\right]_{axis}$; forces circularity at axis.

These determine ϵ_{k_3} and u_{ax}. One can easily plot the level curves of ψ_0 for a fixed set of amplitudes to check the shape of the outermost flux surfaces. We adjust ϵ_{k_2} to minimize the out–of–roundness of the outer surfaces.

As a particular example, we will describe a case where the k's are chosen to be 1, 3, and 13. The optimized amplitudes are then found to be $\epsilon_1 = 1$, $\epsilon_3 = -1.476$, $\epsilon_{13} = -0.49055$, the aspect ratio is 7.60, and the average (cylindrical) normalized radius of the field reversal surface $\lambda\langle\rho_e\rangle = 2.38$ (compared to the infinite aspect ratio value of $j_{0,1} = 2.4048\ldots$). The brackets indicate an average over the poloidal angle. The root-mean-square deviation of the radius of this surface from its mean is 2.0%. The q–profile of this equilibrium agrees well with that of the cylindrically symmetric Bessel function equilibrium.

We now add, as a symmetry-breaking perturbation $\mathbf{B}_1(r,\theta,\phi)$, one term in the series of Eq. (8) with a particular toroidal mode number n. Since this

perturbation also satisfies $\nabla \times \mathbf{B}_1 = \lambda \mathbf{B}_1$, this term represents the effect of a perturbation with toroidal mode number n within the plasma. It is the fully three-dimensional analogue of the magnetic field perturbation given by Eq. (2).

For comparison to an infinite aspect ratio analytic approximation, we determine the island widths by following the field lines in the nonaxisymmetric field $\mathbf{B} = \mathbf{B}_o + \mathbf{B}_1$, in which $\mathbf{B}_o$ is our axisymmetric solution. For $m = 0$ islands, we employ a Poincaré plot in which we plot field line intersections with the midplane $\theta = \pi/2$. This gives two puncture points per revolution around the magnetic axis.

The angle θ_c is no longer an ignorable coordinate in the presence of the perturbation $\mathbf{B}_1$, so no exact flux function ψ_1 for the perturbation can be written down in this case. We find the lowest order approximation to ψ_1 by solving the first order perturbation problem $\mathbf{B}_o \cdot \nabla \psi_1 = -\mathbf{B}_1 \cdot \nabla \psi_0$. Working in the quasi-cylindrical coordinate system (ρ, θ_c, ϕ) and using the cylindrically symmetric Bessel function solution to model $\mathbf{B}_o$, we obtain a relation between ψ_1 and the $m = 0$ component of $B_{1\rho}$ at the field reversal surface:

$$\psi_1(\psi_0 = 0, \theta_c, \phi) \simeq \frac{\lambda^2 R_{ax}^2}{2\pi i n} \psi_0(u = u_{ax}, \theta = \pi/2) \mathrm{J}_1(\lambda \rho_e) \oint \mathrm{B}_{1\rho} d\theta_c \ .$$

Calculation of the latter quantity is facilitated by the relation

$$\frac{1}{2\pi} \oint \mathrm{B}_{1\rho} d\theta_c = -\frac{in}{2\pi R_{ax} \rho_e} \int \int \mathrm{B}_{1\phi} dA \quad ,$$

which follows from the fact that $\mathbf{B}_1$ satisfies $\nabla \times \mathbf{B}_1 = \lambda \mathbf{B}_1$ and has the given ϕ dependence $\exp(in\phi)$. The area integral is estimated in the large aspect ratio limit by evaluating $\mathrm{B}_{1\phi}$ at the magnetic axis and multiplying by $\pi \rho_e^2$. The final result for the normalized full island width at the field reversal surface is then

$$\lambda \Delta_{m=0} \approx 4.30 \left[\frac{u_{ax} \sqrt{\mathbf{Re}^2(\mathrm{B}_{1\phi}|_{ax}) + \mathbf{Im}^2(\mathrm{B}_{1\phi}|_{ax})}}{\psi_0(u = u_{ax}, \vartheta = \pi/2)} \right]^{\frac{1}{2}} \quad ,$$

where

$$\mathrm{B}_{1\phi}|_{ax} = \left. \frac{d\mathrm{P}_k^n(\mu)}{d\mu} \right|_{\mu=0} j_k(u_{ax}) + in \mathrm{P}_k^n(0) \frac{1}{u_{ax}} \left[\frac{d}{du} (u j_k(u)) \right]_{u=u_{ax}} ,$$

and the equilibrium flux function evaluated at the magnetic axis is

$$\psi_0(u = u_{ax}, \theta = \pi/2) = \sum_{k=1}^{\infty} \epsilon_k u_{ax} j_k(u_{ax}) \left. \frac{d\mathrm{P}_k(\mu)}{d\mu} \right|_{\mu=0} .$$

We compare the field line following results with this formula for our example equilibrium as a function of perturbation amplitude in Fig. 6. The simplest infinite aspect ratio calculation predicts the island width within about 15%, which is on the order of the inverse aspect ratio, 0.13. We observe that the island width scales with the square root of the perturbation amplitude in the range of amplitudes considered, thus verifying that nonlinear effects are unimportant in this range. We conclude that the cylindrical approximation is a good one.

V. APPLICATION AND DISCUSSION

We have calculated the widths of the magnetic islands at the field reversal surface in the presence of nonaxisymmetric field errors. The self-consistent plasma response has been included through the assumption that the plasma relaxes to a state described by Eq. (1), with λ a constant. We have seen that the plasma currents can have a large effect on the island widths. To determine the significance of the effects we have discussed, we must estimate the magnitude of the field error we expect to encounter in actual devices, and substitute it into our equations. We do that in this section.

We expect that the toroidal field ripple, an unavoidable consequence of the discreteness of the toroidal field coils, will be an important source of field error in large RFP's. To estimate the magnitude of this error, we model the poloidal current distribution in the toroidal field coils with a sinusoidal current layer localized at $\rho = \rho_C$:

$$\mathbf{J} = \hat{\theta}_c \delta(\rho - \rho_C)\Big(\frac{I_T}{2\pi R}\Big)(1 + \cos n\phi),$$

where I_T is the total poloidal current in the set of n coils. We solve the vacuum field problem by introducing a scalar potential and matching the solution valid for $\rho < \rho_C$ to the solution for $\rho > \rho_C$. For the radial component of the field at $\rho = \rho_e$, we find

$$b_1 = (2 \times 10^{-7})\frac{nI_T}{R}\Big(\frac{\rho_C}{R}\Big)\mathrm{I}_1(n\frac{\rho_e}{R})\mathrm{K}_1(n\frac{\rho_C}{R})$$

in SI units. Note that in this formula I_T is again the total poloidal current, while I_1 is a Bessel function. The magnitude of the poloidal current determines the toroidal flux, which in turn determines B_o. Assuming that the RFP is operated in such a way that the toroidal flux within the plasma ($\rho < \rho_e$) is conserved,

$$\int\int B_\phi dA = 2\pi \mathrm{B}_o \int_0^{\rho_e} \mathrm{J}_0(\lambda\rho)\rho d\rho = 2\pi\frac{\rho_e}{\lambda}\mathrm{B}_o\mathrm{J}_1(\lambda\rho_e) = \pi\rho_e^2(2 \times 10^{-7})\frac{I_T}{R};$$

so defining the toroidal field ripple as the ratio of the radial field at the plasma edge to the toroidal field at the plasma center, we get

$$b_1/B_o = \frac{nJ_1(2\Theta)}{\Theta}\frac{\rho_C}{R}I_1(n\frac{\rho_e}{R})K_1(n\frac{\rho_C}{R}).$$

As a particular example we consider the Los Alamos ZT–H proposal.[12] The proposed device is an RFP with major radius $R = 2.15$ m, liner minor radius $\rho_e = 0.40$ m, with 72 toroidal field coils of mean radius $\rho_C = 0.60$ m. The relatively large number of toroidal field coils has been proposed precisely to minimize the deleterious effects of the toroidal field ripple. Tokamaks, for example, typically have about 20 toroidal field coils. With the 72 coil set the toroidal field ripple of ZT–H would be 0.022% at a pinch parameter of $\Theta = 1.4$. With a more conventional set of 20 toroidal field coils the ripple would be 2.6% at the same pinch parameter.

Using the results of Sec. II, we plot the half-width of the $m = 0$ islands divided by the width of the field reversed layer $(\rho_e - \rho_0)$ as a function of pinch parameter for the 72 coil case and the 20 coil case in Fig. 7. We show three curves on each plot: the width with a distant conducting shell (or on the time scale longer than the shell's resistive time), the width with a shell with radius 5% larger than the plasma edge radius, and the island width calculated ignoring the plasma amplification effect discussed in Sec. II. (This is also the width of the islands on the time scale short compared to the resistive time of the shell in the case of a close–fitting shell.) The curves become singular even for the vacuum case. That is because we are normalizing relative to the width of the field reversal layer, which goes to zero as Θ goes to 1.2. This is, nonetheless, a reasonable normalization to take, because we expect operation of the RFP to be degraded when the island widths become comparable to this field reversal width. The instability which appears just above the field reversal condition $\Theta = 1.2$ for $\rho_w/\rho_e > 1$ narrows the available window for RFP operation; for the cases shown in Fig. 7, where $\rho_w/\rho_e = \infty$, the minimum values of Θ are 1.248 for 72 coils and 1.390 for 20 coils. The minimum operating Θ is increased further by the requirement that the islands on the field reversal surface do not interact significantly with the walls. If we require the island half-width to be less than the width of the field reversal region, $\Theta_{min} = 1.249$ for the 72 coil case and $\Theta_{min} = 1.448$ for the 20 coil case. These results are consistent with the experimental observation that RFP plasmas tend to require Θ significantly higher than 1.2 for field reversal.[9]

Using the large argument asymptotic form of the Bessel functions I_1 and K_1, we find that b_1/B_o depends exponentially on $(\rho_C - \rho_e)$. This implies that our use of the mean toroidal field coil radius in our zero–thickness coil current distribution will yield somewhat narrower islands and less stringent operating requirements than a more realistic coil current distribution would.

The authors of Ref. 12 estimate the magnitude of various vacuum field errors for the ZT–H design. With the field ripple due to the discreteness of the toroidal field coils reduced to a relatively low level by the 72 coil design, they conclude

that the most significant residual field errors are the $n = 1$ error resulting from mechanical tolerances and an $n = 12$ error resulting from the support structure for the torus. Given an estimate for the magnitude of the $m = 0$ components, the methods described in this paper can be easily applied to these field errors as well to estimate the importance of the self-consistent plasma response to these perturbations.

We conclude that the islands driven by field ripple are a significant effect which must be taken into account in designing an RFP. Our results allow the evaluation of the effect for any given level of field ripple. In particular, for the ZT-H device, we find that the proposed use of 72 toroidal field coils does reduce the ripple due to the toroidal field coils to an acceptable level. In this case, the importance of the other known $m = 0$ field perturbations remains to be evaluated.

ACKNOWLEDGMENT

This work was supported by the United States Department of Energy under Contract DE-AC02-76-CHO-3073.

REFERENCES

[1]E. J. Caramana and D. A. Baker, Nucl. Fusion **24**, 423 (1984).

[2]F. W. J. Olver, in *Handbook of Mathematical Functions*, edited by M. Abramowitz and I. Stegun (National Bureau of Standards, Washington, D. C. , 1964), p. 355.

[3]R. S. Massey *et al.*, Los Alamos National Laboratory Report LA-9567-MS, February 1983.

[4]J. B. Taylor, Phys. Rev. Lett. **33**, 1139 (1974).

[5]A. H. Reiman, Phys. Fluids **24**, 956 (1981).

[6]R. Spencer, Proceedings of the Reversed Field Pinch Theory Workshop, Los Alamos National Laboratory Report LA-8944-C, 129 (1981).

[7]R. B. Howell and H. F. Vogel, J. Appl. Phys. **56**, 2017 (1984).

[8]R. D. Gibson and K. J. Whiteman, Plasma Phys. **10**, 1101 (1968).

[9]H. A. B. Bodin and A. A. Newton, Nucl. Fusion **20**, 1255 (1980).

[10]W. A. Newcomb, Ann. Phys. **10**, 232 (1960).

[11]M. N. Rosenbluth and M. N. Bussac, Nucl. Fusion **19**, 489 (1979).

[12]D. Baker, C. Bathke *et al.* , *ZT-H Reversed Field Pinch Experiment Technical Proposal*, Los Alamos National Laboratory Report LA-UR-84-2602, June 1984.

FIGURES

FIG. 1. The amplification factor for response to an $n = 20$, $m = 0$ perturbation, as a function of the pinch parameter Θ. The nature of the instability which occurs below a critical value of Θ is also indicated. Aspect ratio $R/\rho_e = 5.7$, no conducting shell.

FIG. 2. Amplification factor for response to an $n = 72$, $m = 0$ perturbation. Aspect ratio $R/\rho_e = 5.7$, no conducting shell.

FIG. 3. Amplification factor for response to an $n = 20$, $m = 0$ perturbation, with a conducting shell 5% larger in radius than the plasma. Aspect ratio $R/\rho_e = 5.7$.

FIG. 4. Stability diagram for $m = 0$ tearing modes, aspect ratio $R/\rho_e = 5.7$. The solid line indicates the marginal point $\Delta' = 0$, and the dashed line represents an asymptotic expansion good for $N \gg 14$.

FIG. 5. Stability diagram for $m = 0$ tearing modes, aspect ratio $R/\rho_e = 5.7$. Three marginal stability curves are shown: one for a close–fitting conducting shell (no vacuum region), one for no conducting shell, and the intermediate case with a conducting shell 15% larger in radius than the plasma.

FIG. 6. Comparison of $m = 0$, $n = 2$ island width in a toroidal equilibrium predicted by the cylindrical approximation (dashed line) with the width obtained from numerical field line following (solid line), as a function of perturbation amplitude. The width is normalized by the eigenvalue of Eq. (1), λ.

FIG. 7. Half–width of $m = 0$ islands, normalized by $(\rho_e - \rho_0)$ as a function of the pinch parameter Θ, for ZT–H. In both plots, the plasma aspect ratio $R/\rho_e = 5.375$, and the coil aspect ratio $R/\rho_C = 3.583$. The solid lines indicate the island width with no conducting shell, the dashed lines show the width with a shell of radius $\rho_w = 1.05\rho_e$, and the chain dashed lines show the width with a close fitting shell. The latter case also is the island width one would obtain ignoring the self–consistent plasma amplification effect.

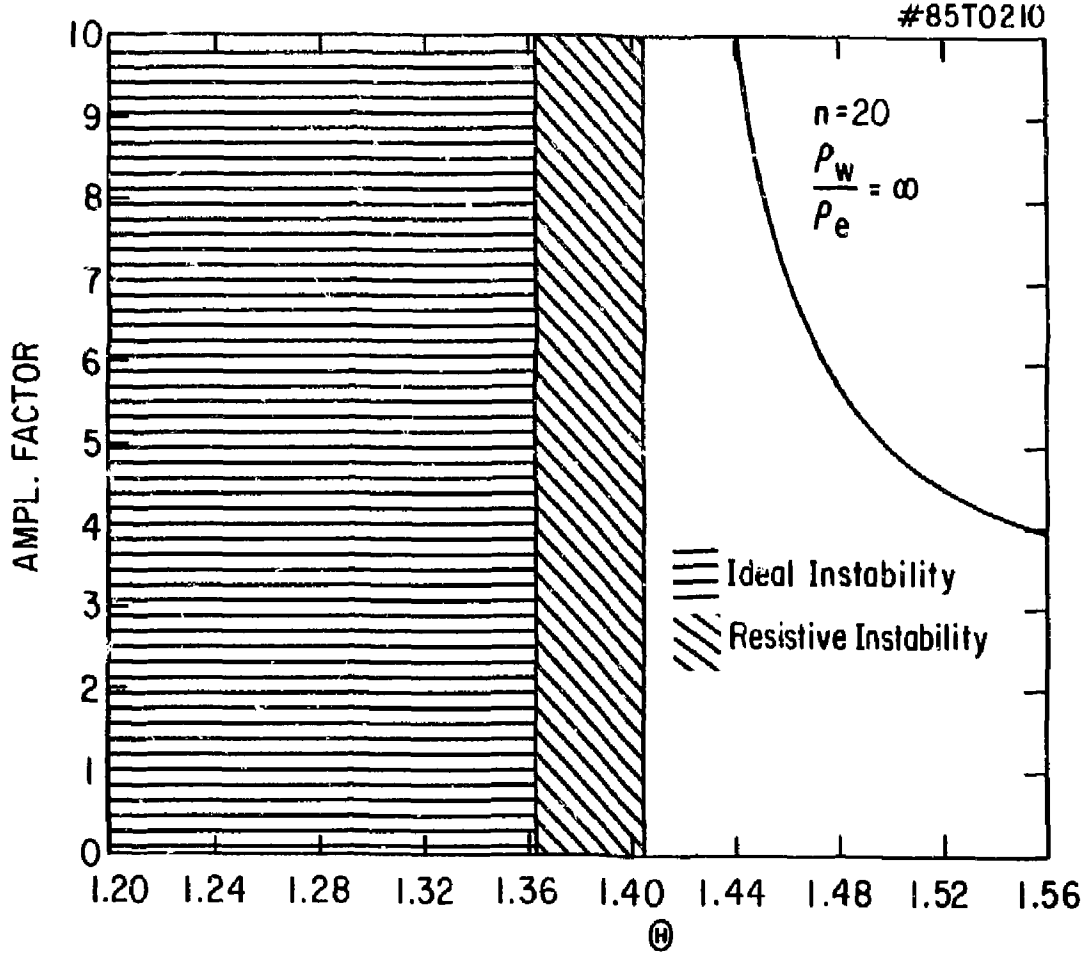
#85T0210
AMPL. FACTOR
10
9
8
7
6
5
4
3
2
1
0
n=20
$\frac{\rho_w}{\rho_e} = \infty$
Ideal Instability
Resistive Instability
1.20
1.24
1.28
1.32
1.36
1.40
1.44
1.48
1.52
1.56
Θ

Fig. 1

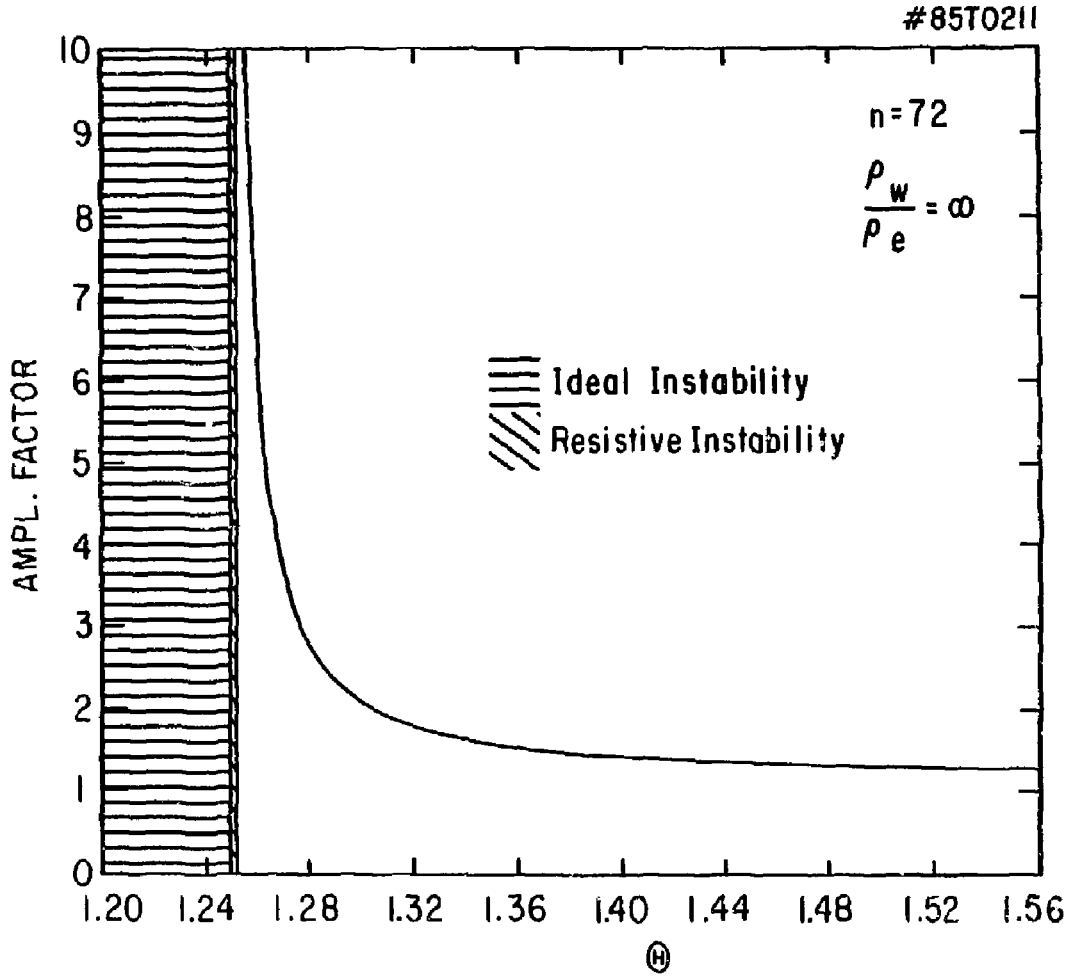
#85T0211
n=72
$\frac{\rho_w}{\rho_e} = \infty$
Ideal Instability
Resistive Instability
AMPL. FACTOR
0
1
2
3
4
5
6
7
8
9
10
1.20
1.24
1.28
1.32
1.36
1.40
1.44
1.48
1.52
1.56
Θ

Fig. 2

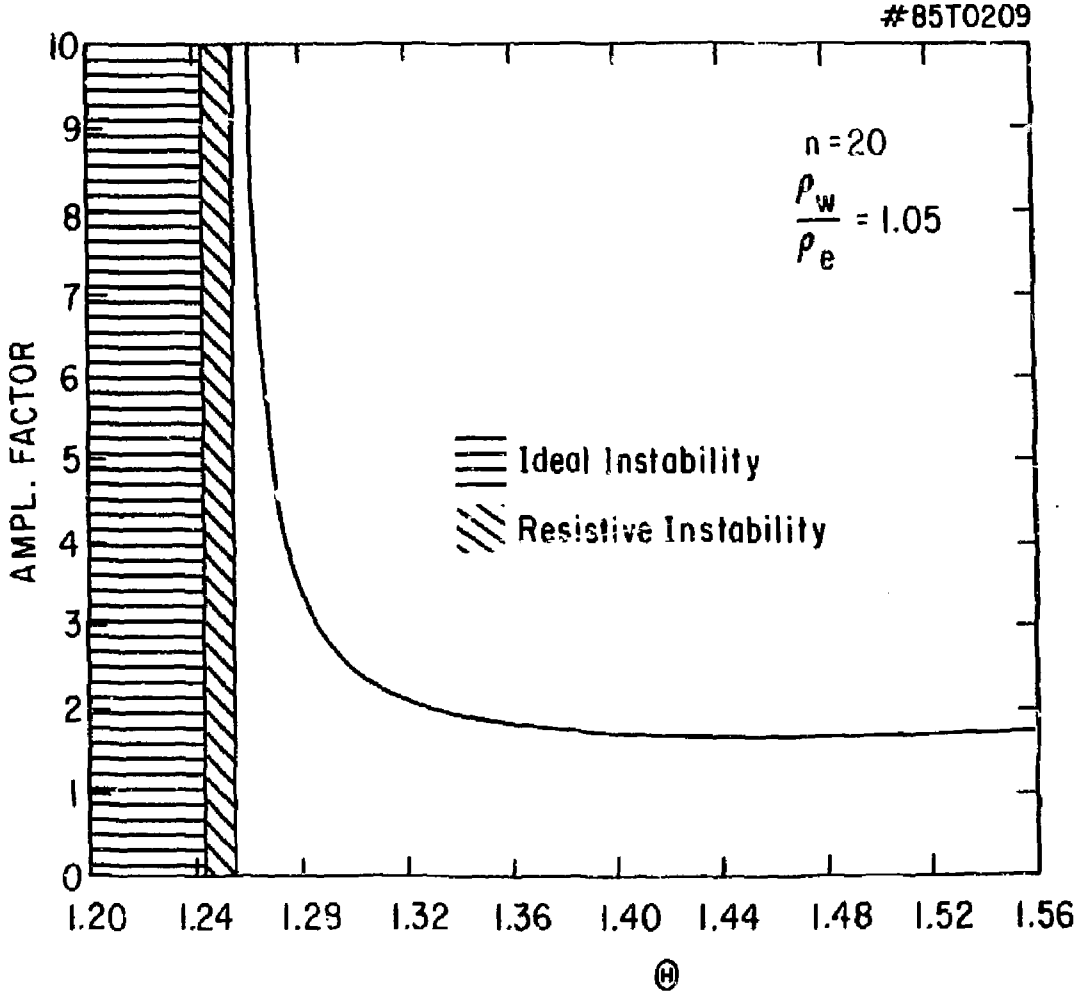
#85T0209
AMPL. FACTOR
10
9
8
7
6
5
4
3
2
1
0
n = 20
$\frac{\rho_w}{\rho_e}$ = 1.05
Ideal Instability
Resistive Instability
1.20
1.24
1.29
1.32
1.36
1.40
1.44
1.48
1.52
1.56
Ⓗ

Fig. 3

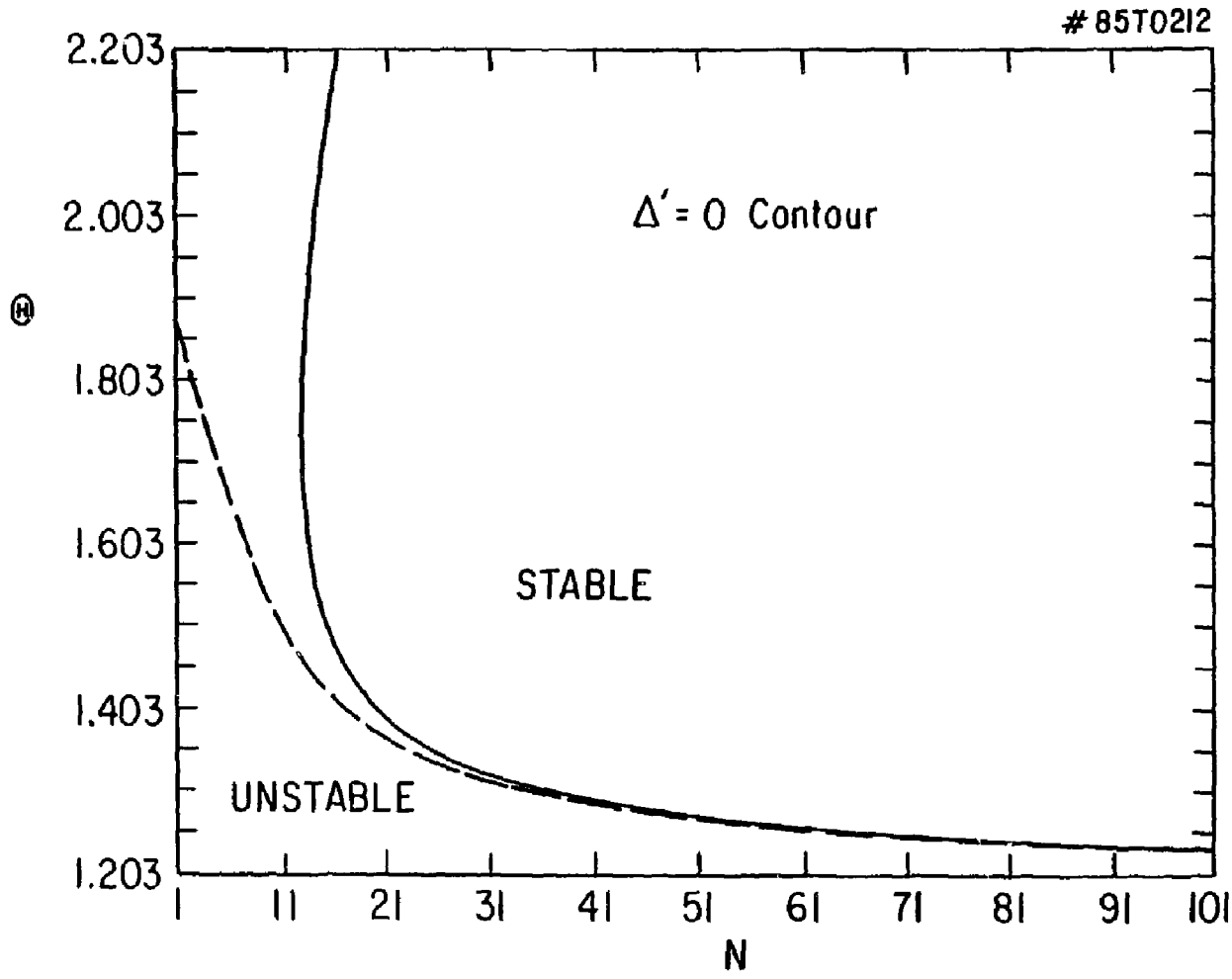
#85T0212
2.203
2.003
1.803
1.603
1.403
1.203
Ⓗ
Δ′ = 0 Contour
STABLE
UNSTABLE
1
11
21
31
41
51
61
71
81
91
101
N

Fig. 4

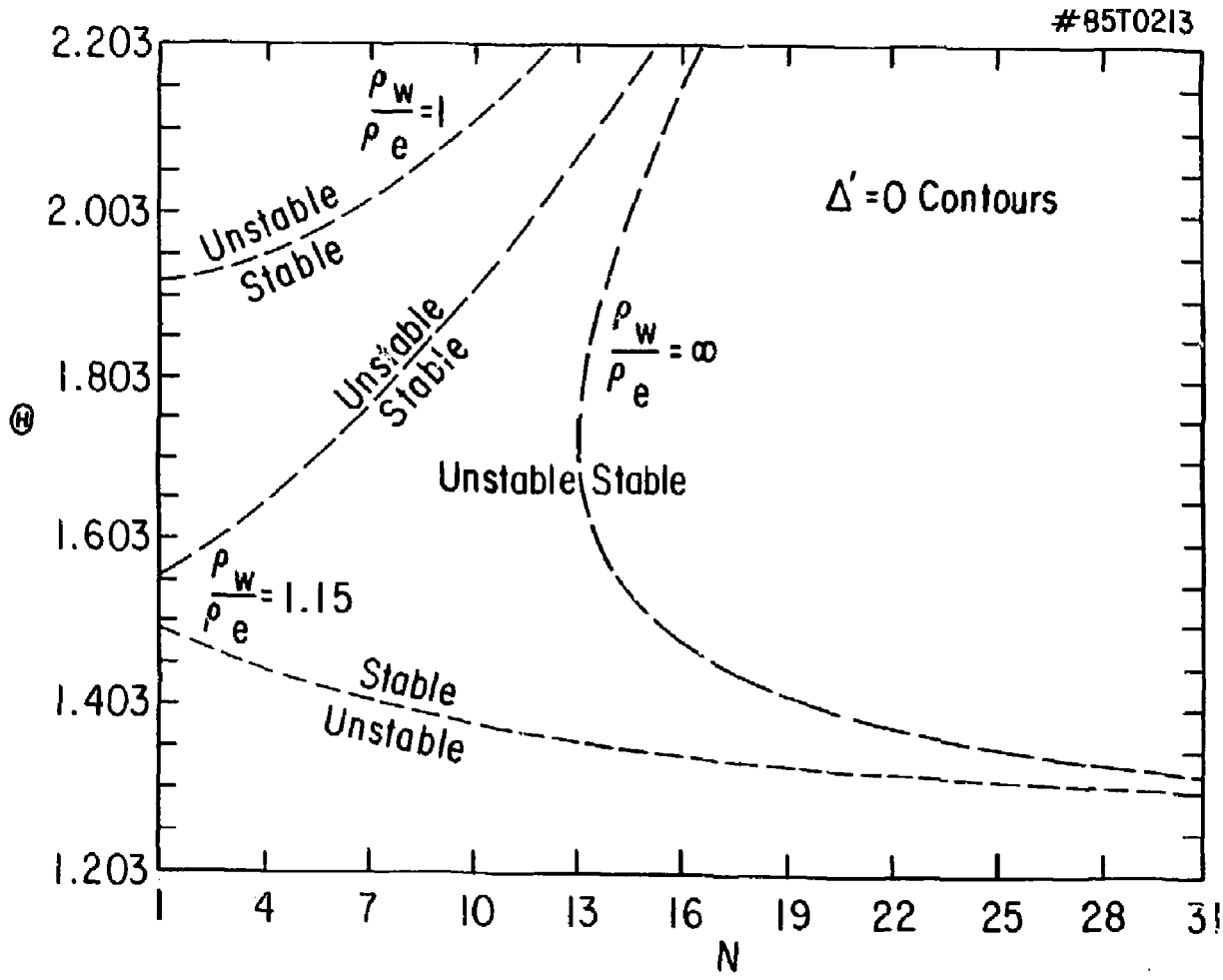
#85T0213
2.203
2.003
1.803
1.603
1.403
1.203
Θ
1
4
7
10
13
16
19
22
25
28
31
N
Δ′=0 Contours
ρw/ρe=1
Unstable
Stable
ρw/ρe=1.15
Stable
Unstable
ρw/ρe=∞
Unstable
Stable
Unstable
Stable

Fig. 5

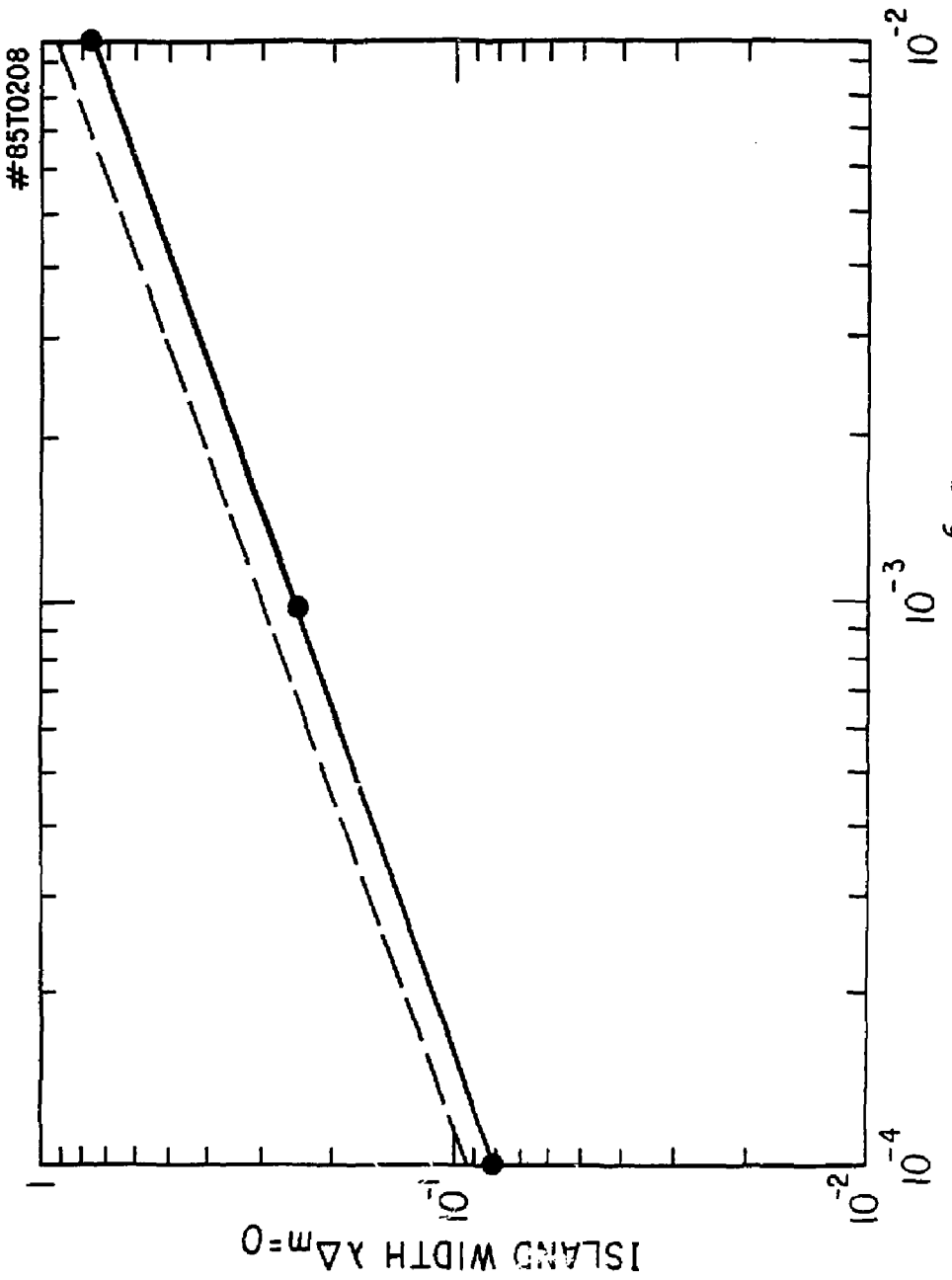
#65T0208
ISLAND WIDTH $\lambda\Delta_{m=0}$
ϵ_{23}
10^{-1}
10^{-2}
10^{-3}
10^{-4}

Fig. 6

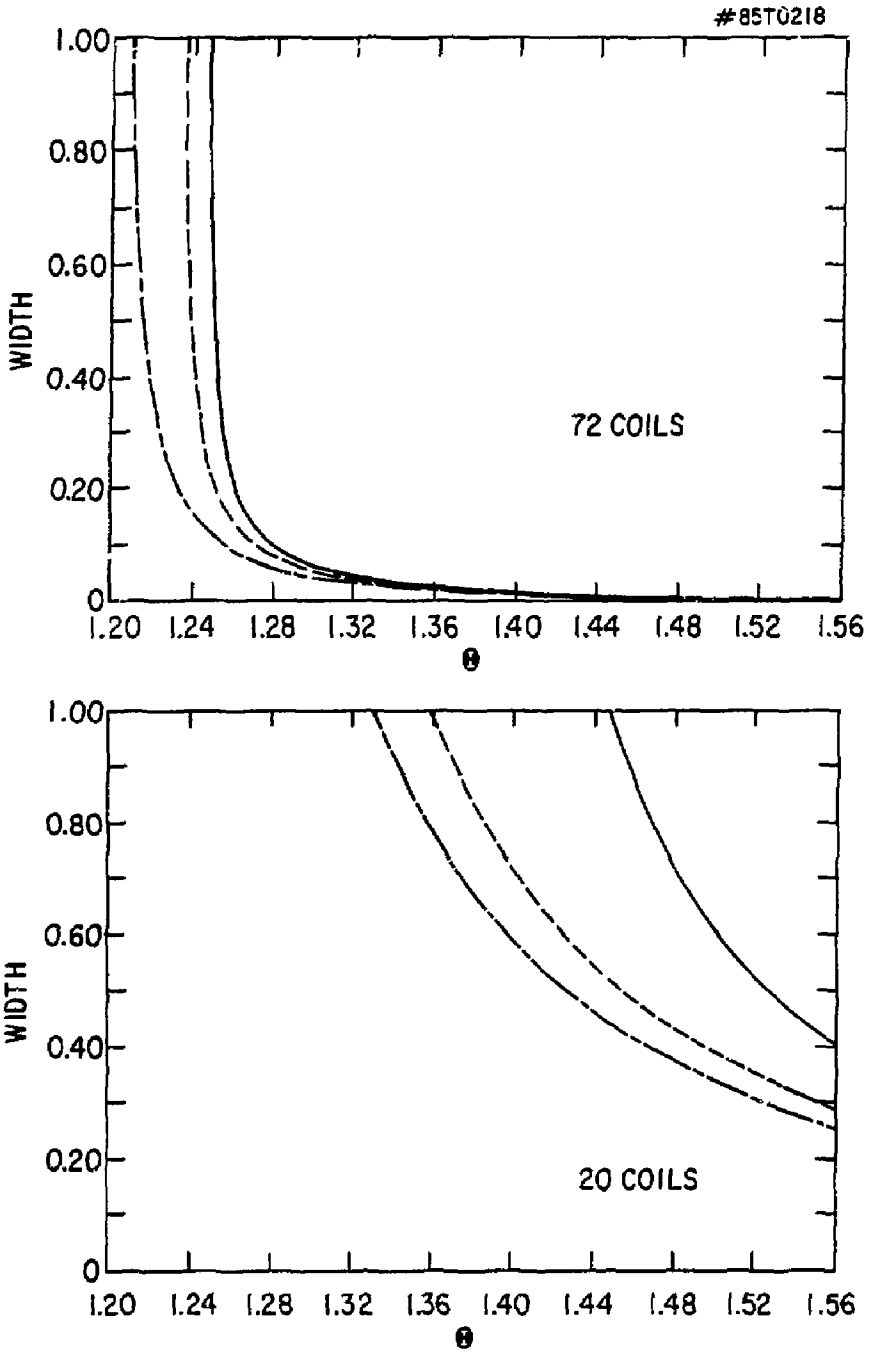
#85T0218
1.00
0.80
0.60
0.40
0.20
0
WIDTH
72 COILS
1.20 1.24 1.28 1.32 1.36 1.40 1.44 1.48 1.52 1.56
θ
1.00
0.80
0.60
0.40
0.20
0
WIDTH
20 COILS
1.20 1.24 1.28 1.32 1.36 1.40 1.44 1.48 1.52 1.56
θ

Fig. 7

EXTERNAL DISTRIBUTION IN ADDITION TO UC-20

Plasma Res Lab, Austra Nat'l Univ, AUSTRALIA
Dr. Frank J. Paoloni, Univ of Wollongong, AUSTRALIA
Prof. I.R. Jones, Flinders Univ., AUSTRALIA
Prof. M.H. Brennan, Univ Sydney, AUSTRALIA
Prof. F. Cap, Inst Theo Phys, AUSTRIA
Prof. Frank Verheest, Inst theoretische, BELGIUM
Dr. D. Palumbo, Dg XII Fusion Prog, BELGIUM
Ecole Royale Militaire, Lab de Phys Plasmas, BELGIUM
Dr. P.H. Sakanaka, Univ Estadual, BRAZIL
Dr. C.R. James, Univ of Alberta, CANADA
Prof. J. Teichmann, Univ of Montreal, CANADA
Dr. H.M. Skarsgard, Univ of Saskatchewan, CANADA
Prof. S.R. Sreenivasan, University of Calgary, CANADA
Prof. Tudor W. Johnston, INRS-Energie, CANADA
Dr. Hannes Barnard, Univ British Columbia, CANADA
Dr. M.P. Bachynski, MPB Technologies, Inc., CANADA
Chalk River, Nucl Lab, CANADA
Zhengwu Li, SW Inst Physics, CHINA
Library, Tsing Hua University, CHINA
Librarian, Institute of Physics, CHINA
Inst Plasma Phys, Academia Sinica, CHINA
Dr. Peter Lukac, Komenskeho Univ, CZECHOSLOVAKIA
The Librarian, Culham Laboratory, ENGLAND
Prof. Schatzman, Observatoire de Nice, FRANCE
J. Radet, CEN-BP6, FRANCE
AM Dupas Library, AM Dupas Library, FRANCE
Dr. Tom Mual, Academy Bibliographic, HONG KONG
Preprint Library, Cent Res Inst Phys, HUNGARY
Dr. S.K. Trehan, Panjab University, INDIA
Dr. Indra Mohan Lal Das, Banaras Hindu Univ, INDIA
Dr. L.K. Chavda, South Gujarat Univ, INDIA
Dr. R.K. Chhajlani, Vikram Univ. INDIA
Dr. B. Dasgupta, Saha Inst, INDIA
Dr. P. Kaw, Physical Research Lab, INDIA
Dr. Phillip Rosenau, Israel Inst Tech, ISRAEL
Prof. S. Cuperman, Tel Aviv University, ISRAEL
Prof. G. Rostagni, Univ Di Padova, ITALY
Librarian, Int'l Ctr Theo Phys, ITALY
Miss Clelia De Palo, Assoc EURATOM-ENEA, ITALY
Biblioteca, del CNR EURATOM, ITALY
Dr. H. Yamato, Toshiba Res & Dev, JAPAN
Direc. Dept. Lg. Tokamak Dev. JAERI, JAPAN
Prof. Nobuyuki Inoue, University of Tokyo, JAPAN
Research Info Center, Nagoya University, JAPAN
Prof. Kyoji Nishikawa, Univ of Hiroshima, JAPAN
Prof. Sigeru Mori, JAERI, JAPAN
Library, Kyoto University, JAPAN
Prof. Ichiro Kawakami, Nihon Univ, JAPAN
Prof. Satoshi Itoh, Kyushu University, JAPAN
Dr. D.I. Choi, Adv. Inst Sci & Tech, KOREA
Tech Info Division, KAERI, KOREA
Bibliotheek, Fom-Inst Voor Plasma, NETHERLANDS
Prof. B.S. Liley, University of Waikato, NEW ZEALAND
Prof. J.A.C. Cabral, Inst Superior Tecn, PORTUGAL
Dr. Octavian Petrus, ALI CUZA University, ROMANIA
Prof. M.A. Hellberg, University of Natal, SO AFRICA
Dr. Johan de Villiers, Plasma Physics, Nucor, SO AFRICA
Fusion Div. Library, JEN, SPAIN
Prof. Hans Wilhelmson, Chalmers Univ Tech, SWEDEN
Dr. Lennart Stenflo, University of UMEA, SWEDEN
Library, Royal Inst Tech, SWEDEN
Centre de Recherchesen, Ecole Polytech Fed, SWITZERLAND
Dr. V.T. Tolok, Kharkov Phys Tech Ins, USSR
Dr. D.D. Ryutov, Siberian Acad Sci, USSR
Dr. G.A. Eliseev, Kurchatov Institute, USSR
Dr. V.A. Glukhikh, Inst Electro-Physical, USSR
Institute Gen. Physics, USSR
Prof. T.J.M. Boyd, Univ College N Wales, WALES
Dr. K. Schindler, Ruhr Universitat, W. GERMANY
Nuclear Res Estab, Julich Ltd, W. GERMANY
Librarian, Max-Planck Institut, W. GERMANY
Bibliothek, Inst Plasmaforschung, W. GERMANY
Prof. R.K. Janev, Inst Phys, YUGOSLAVIA